

SEARCH FOR THE SIGNATURES OF THE DECONFINED STATE OF
 HADRONIC MATTER IN \bar{p} - p INTERACTIONS AT
 $\sqrt{s} = 300, 546, 1000, \text{ and } 1800 \text{ GeV}$

presented by
 Laszlo J. Gutay

T. Alexopoulos, C. Allen, E.W. Anderson, V. Balamurali, S. Banerjee, P.D. Beery, P. Bhat, J.M. Bishop, N.N. Biswas,
 A. Bujak, D.D. Carmony, T. Carter, Y. Choi, P. Cole, R. De Bonte, V. De Carlo, A.R. Erwin, C. Fineisen, A.T. Goshaw, L.J. Gutay,
 A.S. Hirsch, C. Hojvat, J.R. Jennings, V.P. Kenny, C.S. Lindsey, C. Loomis, J.M. LoSecco, T. McMahon, A.P. McManus, N.
 Morgan, K. Nelson, S.H. Oh, N.T. Porile, D. Reeves, A. Rimai, W. J. Robertson, R.P. Scharenberg, S.R. Stampke, B.C.
 Stringfellow, M. Thompson, F. Turkot, W.D. Walker, C.H. Wang, J. Warchol, D.K. Wesson and Y. Zhan

(FNAL C0 E735 Collaboration)

I. Introduction

It is anticipated theoretically that at sufficiently high energy density ($\sim 2 \text{ GeV/f}^3$) particles deconfine into quarks. Thus a vapor (particle) - liquid (quark) first order phase transition may take place. This prediction has experimental relevance only if such a phase transition has observable consequences. Since we can describe phase transition only in terms of thermodynamic variables, we assume that such a description is applicable. Thus we will attempt to describe a short lived and finite size system which decays into multiparticle final state in terms of Entropy (S), Temperature (T) and Pressure (P). Further, knowing empirically the T-S phase diagram for hydrogen at the vapor-liquid phase transition region, we will look for similar behavior in \bar{p} - p collisions. Once the deconfined state is formed it will behave as a radiating and expanding system. Using theoretical assumptions of varying reliability and expecting similarity between behavior of hadronic and molecular systems at phase transition, we can enumerate the expected deconfinement signatures:

- (a) First order phase transition in the T-S plane
- (b) Enhancement of baryonic antimatter production
- (c) Strange particle enhancement

- (d) Sudden change in Backward-Forward correlations
- (e) Break down of KNO scaling at large multiplicity
- (f) Emergence of transverse flow
- (g) Enhancement of low energy photon and low effective mass lepton pair production

II. Experimental Evidence for Hadron Thermodynamics

Classical results of thermodynamics and statistical mechanics were derived assuming infinite systems in thermal equilibrium. Thus applying thermodynamics to short lived subatomic systems was met with considerable skepticism. However a series of experiments have shown that using statistical methods, a meaningful value can be obtained for the temperature, size, and the lifetime of the Centrally Produced Hadronic Radiator in p-p collisions. The indisputable proof however came from p-nucleus collisions.

In high energy ($20 \text{ GeV}/c < p < 400 \text{ GeV}/c$) proton-Xenon collision the yields of fragment was measured.



As shown in Figure 1, the fragment yield fell as $A^{-2.6}$ where A denotes the nucleon number of the fragment. We interpreted the above experimental result as a manifestation of critical behavior of strongly interacting matter. This interpretation is based on the empirical observation that in the neighborhood of the critical point the cluster size distribution has a power law form $\ell^{-\tau}$, where ℓ denotes the number of constituents of the cluster and $2 < \tau < 3$ for a three dimensional system. Using a gold beam recently two more critical indexes γ and β have been determined. Their values are in agreement with theoretical expectations, and satisfy the relation which connects them.

III. Thermodynamical Variables, Relevant for Quark Deconfinement

To prove the applicability of the concept of critical behavior to nuclear fragmentation, we used variables which were directly measurable. To apply thermodynamics to quark deconfinement we must identify T and S with quantities measurable in deep inelastic $\bar{p} - p$ collisions. We made the identifications:

$$S \sim dn/d\eta \text{ (particle rapidity density)}$$

$$T \sim \langle p_t \rangle \text{ (average transverse momentum)}$$

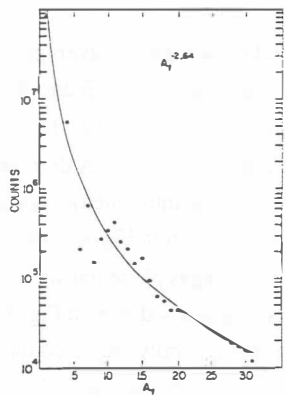


Fig.: 1 Mass yields of fragments from xenon vs mass number, A_f .

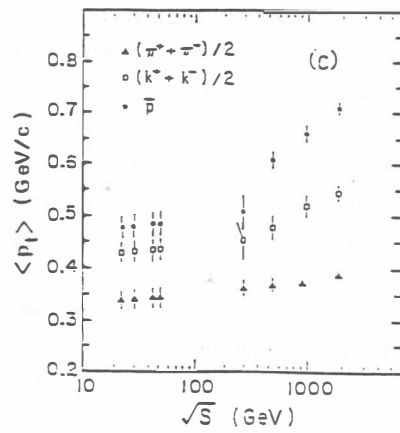


Fig.: 2c The energy dependence of the $\langle p_t \rangle$ for π , K and \bar{p} .

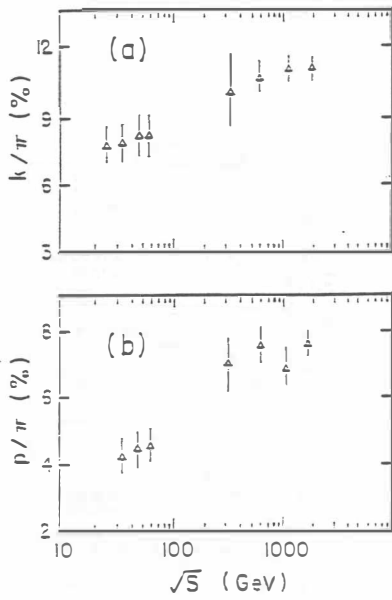


Fig.: 2a The energy dependence of the K/π ratios.

2b The energy dependence of the \bar{p}/π ratios.

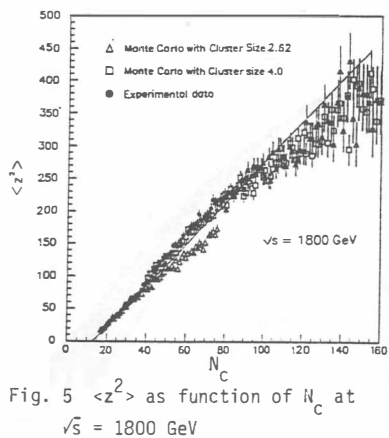


Fig. 5 $\langle z^2 \rangle$ as function of N_c at $\sqrt{s} = 1800$ GeV

IV. Experimental Results

In Figs. 2a - 2c the energy dependence of particle ratios and the average transverse momentum is shown. A clear rise in the relative amount of \bar{p} and K^\pm production and dramatic increase in the $\langle p_t \rangle$ is observed above 300 GeV. In Fig. 3 the energy dependence of the scaled multiplicity distribution is shown. A dramatic deviation from scaling develops above 300 GeV. The charged multiplicity dependence of the average transverse momentum for π , K and \bar{p} are shown in Fig. 4. Note the increase and flattening of $\langle p_t \rangle$ resembles the shape of liquid gas phase transition curve. The variance of the forward-backward multiplicity distribution is shown in Fig. 5. The slope of the curve is related to the number of particles the centrally produced clusters decay. Note the upturn about $n_c \sim 40$ indicating an increase in cluster size. We have found no evidence for low energy photon enhancement, but there is a hint of transverse flow at large n_c .

In conclusion, the energy and multiplicity dependence of several measurable quantities is consistent with what is expected in hadron-quark phase transition.

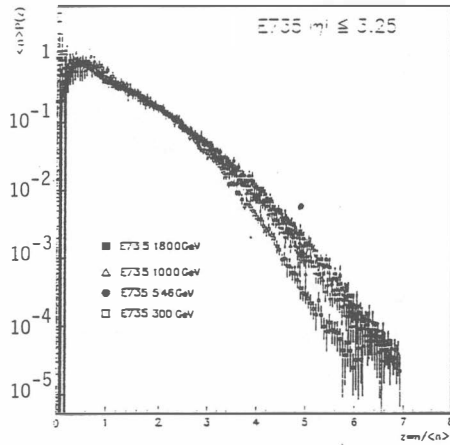


Fig. 3 Normalized multiplicity distributions at four values of \sqrt{s}

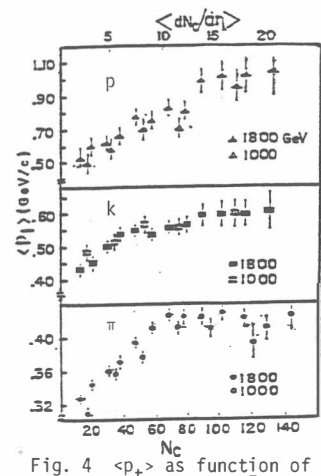


Fig. 4 $\langle p_t \rangle$ as function of N_c for π , k and \bar{p}